



Fabrication and performance of $\text{BaCe}_{0.8}\text{Y}_{0.2}\text{O}_{3-\delta}$ – $\text{BaZr}_{0.8}\text{Y}_{0.2}\text{O}_{3-\delta}$ bilayer electrolyte for anode-supported solid oxide fuel cells



Jing Qian^a, Wenping Sun^a, Qingping Zhang^a, Guoshun Jiang^a, Wei Liu^{a,b,*}

^aCAS Key Laboratory for Energy Conversion & Collaborative Innovation Center of Suzhou Nano Science and Technology, University of Science and Technology of China, Hefei, Anhui 230026, PR China

^bKey Laboratory of Materials Physics, Institute of Solid State Physics, Chinese Academy of Sciences, Hefei 230031, China

HIGHLIGHTS

- Fabricate thin BZY layer on BCY half-cell with pulsed laser deposition.
- The bilayer electrolyte proves a good chemical stability against CO_2 atmosphere.
- The bilayer cell exhibits a good long-term stability under cell testing condition.
- The bilayer electrolyte cell shows a comparable electrochemical performance.

ARTICLE INFO

Article history:

Received 29 July 2013

Received in revised form

21 October 2013

Accepted 25 October 2013

Available online 4 November 2013

Keywords:

Pulsed laser deposition

Bilayer electrolyte

Chemical stability

Cell performance

ABSTRACT

$\text{BaZr}_{0.8}\text{Y}_{0.2}\text{O}_{3-\delta}$ (BZY) layers with various thicknesses (~ 0.7 , ~ 1.7 , ~ 2.4 and ~ 3.6 μm) are fabricated using the pulsed laser deposition (PLD) technique on anode-supported $\text{BaCe}_{0.8}\text{Y}_{0.2}\text{O}_{3-\delta}$ (BCY) electrolyte films. $\text{Sm}_{0.5}\text{Sr}_{0.5}\text{CoO}_{3-\delta}$ -SDC (SSC-SDC, 70:30 wt.%) cathode is applied onto the BZY/BCY bilayer electrolyte to form a single cell. The chemical stability of the BZY/BCY bilayer electrolytes improves with increasing BZY layer thickness. The BZY (~ 3.6 μm)/BCY bilayer electrolyte shows an excellent chemical stability after treated in 100% CO_2 atmosphere at 900 °C. The maximum power densities of 447, 370, 276, 218 and 163 mW cm^{-2} are measured with the BZY layer thicknesses of 0, 0.7, 1.7, 2.4 and 3.6 μm at 700 °C, respectively. In general, the BZY/BCY bilayer electrolyte cell with an optimum BZY layer thickness can improve chemical stability without great influence on the electrochemical performance for intermediate temperature solid oxide fuel cells.

© 2013 Elsevier B.V. All rights reserved.

1. Introduction

High temperature proton conductors (HTPCs) have been extensively investigated since Iwahara et al. have reported some perovskite materials with excellent protonic conductivity at elevated temperatures [1–3]. HTPCs are considered to be the promising electrolyte candidates for intermediate temperature solid oxide fuel cells (IT-SOFCs) due to their larger ionic conductivities and smaller activation energies than conventional oxygen-ion conducting electrolytes [4,5]. Besides, HTPCs form water at the cathode side and thus fuel at the anode side remains pure without recirculation [1]. Acceptor-doped BaCeO_3 and BaZrO_3 compounds have been studied as the promising proton conductors

[6–9]. However, the balance between high proton conductivity and chemical stability seems to be a challenge. Acceptor-doped BaCeO_3 has a high proton conductivity but shows a poor chemical stability in H_2O and CO_2 -containing atmospheres. Doped- BaZrO_3 materials have a high chemical stability. However, the BaZrO_3 -based materials show a low proton conductivity due to the high grain boundary resistance [10,11]. In order to find a compromise between proton conductivity and chemical stability, one effective approach is to incorporate a thin doped- BaZrO_3 film as a protecting layer between BaCeO_3 electrolyte and cathode. However, the doped- BaZrO_3 layer thickness can increase ohmic loss due to the lower proton conductivity compared with that of BaCeO_3 . Thus the BaZrO_3 layer thickness is a key factor in balancing proton conductivity and chemical stability. The pulsed laser deposition (PLD) technique can exactly control film thickness. Besides, it is a promising method to deposit thin films that are of high quality and stoichiometric with multi-component materials [12]. Furthermore, films deposited by PLD do not require high annealing temperatures

* Corresponding author. CAS Key Laboratory of Materials for Energy Conversion, University of Science and Technology of China, Hefei, Anhui 230026, PR China. Tel.: +86 551 63606929; fax: +86 551 63602586.

E-mail address: wliu@ustc.edu.cn (W. Liu).

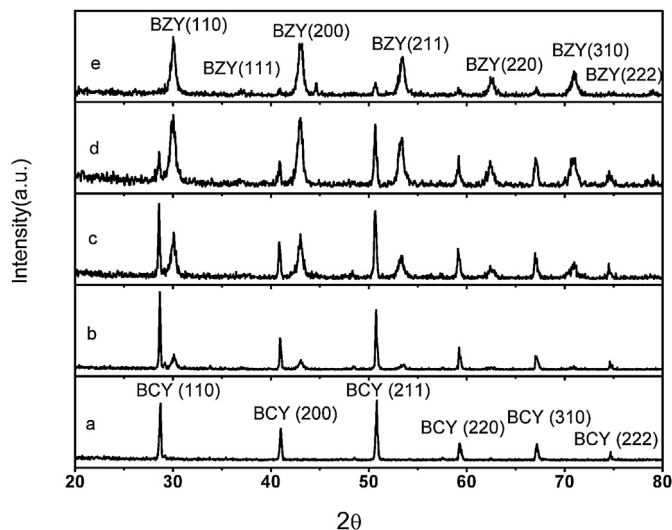


Fig. 1. XRD patterns of (a) BCY single layer, (b) ~ 700 nm BZY/BCY bilayer, (c) ~ 1.7 μm BZY/BCY bilayer, (d) ~ 2.4 μm BZY/BCY bilayer and (e) ~ 3.6 μm BZY/BCY bilayer.

[13], which is useful for low temperature SOFCs applications and avoids the formation of a solid solution between BaZrO_3 and BaCeO_3 . Fabbri et al. [14] have successfully fabricated a proton conductor bilayer electrolyte cell with a thin $\text{BaZr}_{0.8}\text{Y}_{0.2}\text{O}_{3-\delta}$ (BZY) layer deposited on a sintered $\text{BaCe}_{0.8}\text{Y}_{0.2}\text{O}_{3-\delta}$ (BCY) pellet using PLD technique. There are two disadvantages in their work. First, the BCY electrolyte-supported fuel cell increased the ohmic loss compared to the anode-supported fuel cell. Besides, the use of Pt electrodes on the BZY/BCY bilayer electrolyte impeded better electrochemical performance. Therefore, it is necessary to fabricate an anode-supported proton conductor bilayer electrolyte cell. In this work, we fabricated thin BZY layers on a $\text{NiO}-\text{BaZr}_{0.1}\text{Ce}_{0.7}\text{Y}_{0.2}\text{O}_{3-\delta}$ (BZCY)/BCY half-cell using the PLD technique. The thickness of the BZY layer is controlled from ~ 700 nm to ~ 3.6 μm to study the effect of BZY layer thickness on the chemical stability and overall performance of the bilayer electrolyte cells.

2. Experimental

2.1. Powder synthesis and cell fabrication

BCY and BZCY powders were fabricated using a citric acid-nitrate gel combustion process [15]. First, BaCO_3 , $\text{Ce}(\text{NO}_3)_4 \cdot 4\text{H}_2\text{O}$,

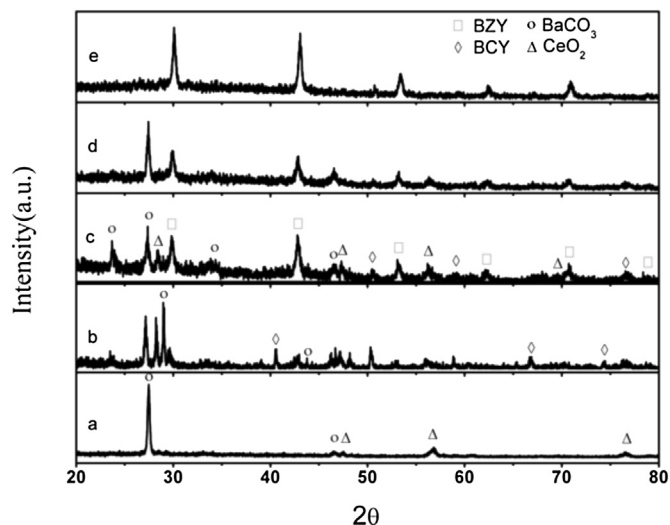


Fig. 3. XRD patterns of anode-supported electrolytes after treatment in CO_2 atmosphere: (a) BCY single layer, (b) ~ 700 nm BZY/BCY bilayer, (c) ~ 1.7 μm BZY/BCY bilayer, (d) ~ 2.4 μm BZY/BCY bilayer and (e) ~ 3.6 μm BZY/BCY bilayer.

$\text{Zr}(\text{NO}_3)_4 \cdot 5\text{H}_2\text{O}$ and $\text{Y}(\text{NO}_3)_3 \cdot 6\text{H}_2\text{O}$ was added to a solution of HNO_3 . After the solution became clear, citric acid was added in a 1:1.5 metal ions:citric acid molar ratio. The pH value was adjusted to approximately 7 with ammonia. The solution was continuously stirred and heated at 70 $^\circ\text{C}$ until a gel formed. The gel was then heated on a hot plate and combusted to form powder precursors, which were then calcined at 1000 $^\circ\text{C}$ for 3 h to obtain a pure, crystalline BCY and BZCY phase. NiO (basic nickel carbonate decomposed at 600 $^\circ\text{C}$) and BZCY were mixed by ball milling in ethanol for 24 h in a weight ratio of 60/40 with 10 wt.% of starch as pore formers. The mixture was dried in an oven at 60 $^\circ\text{C}$ and prepared as anode supporting substrates.

The anode supporting half-cells were fabricated using the co-pressing method. The NiO -BZCY mixed powders were uniaxially pressed to form anode supports with a certain mechanical strength. Then, the as-prepared BCY powders were well distributed on the anode substrates and pressed to fabricate the BCY electrolyte layer. Finally, the anode supporting half-cells were sintered at 1400 $^\circ\text{C}$ for 5 h. The thickness of BCY electrolyte layer is ~ 29 μm .

The thin BZY layer was deposited on the BCY half-cells by ablating a BZY target (fabricated by citric combustion process [15]) and sintered at 1550 $^\circ\text{C}$ for 8 h) with a KrF excimer laser

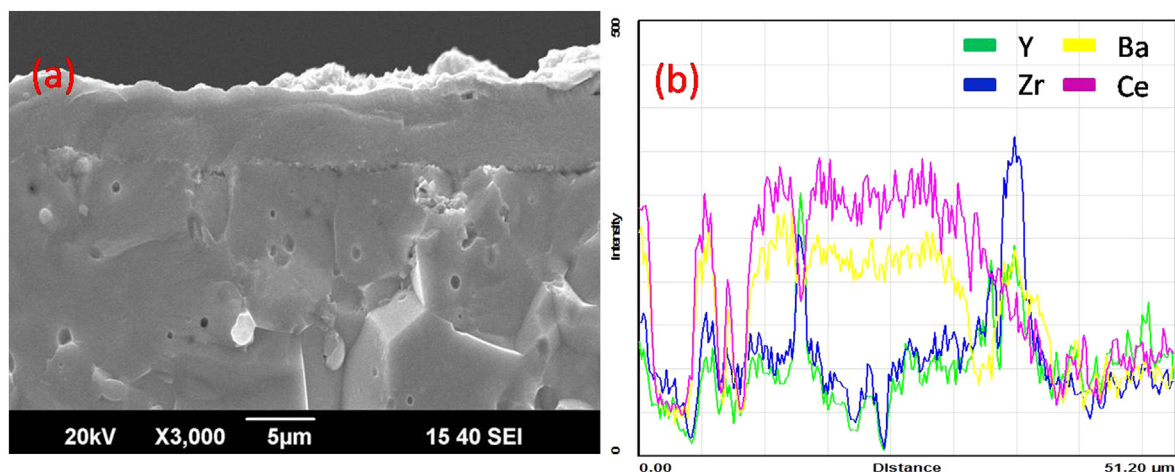


Fig. 2. (a) Cross-sectional view of a BZY/BCY bilayer electrolyte cell, (b) EDS scans as the sequence: anode/BCY electrolyte/BZY/SSC-SDC cathode cell.

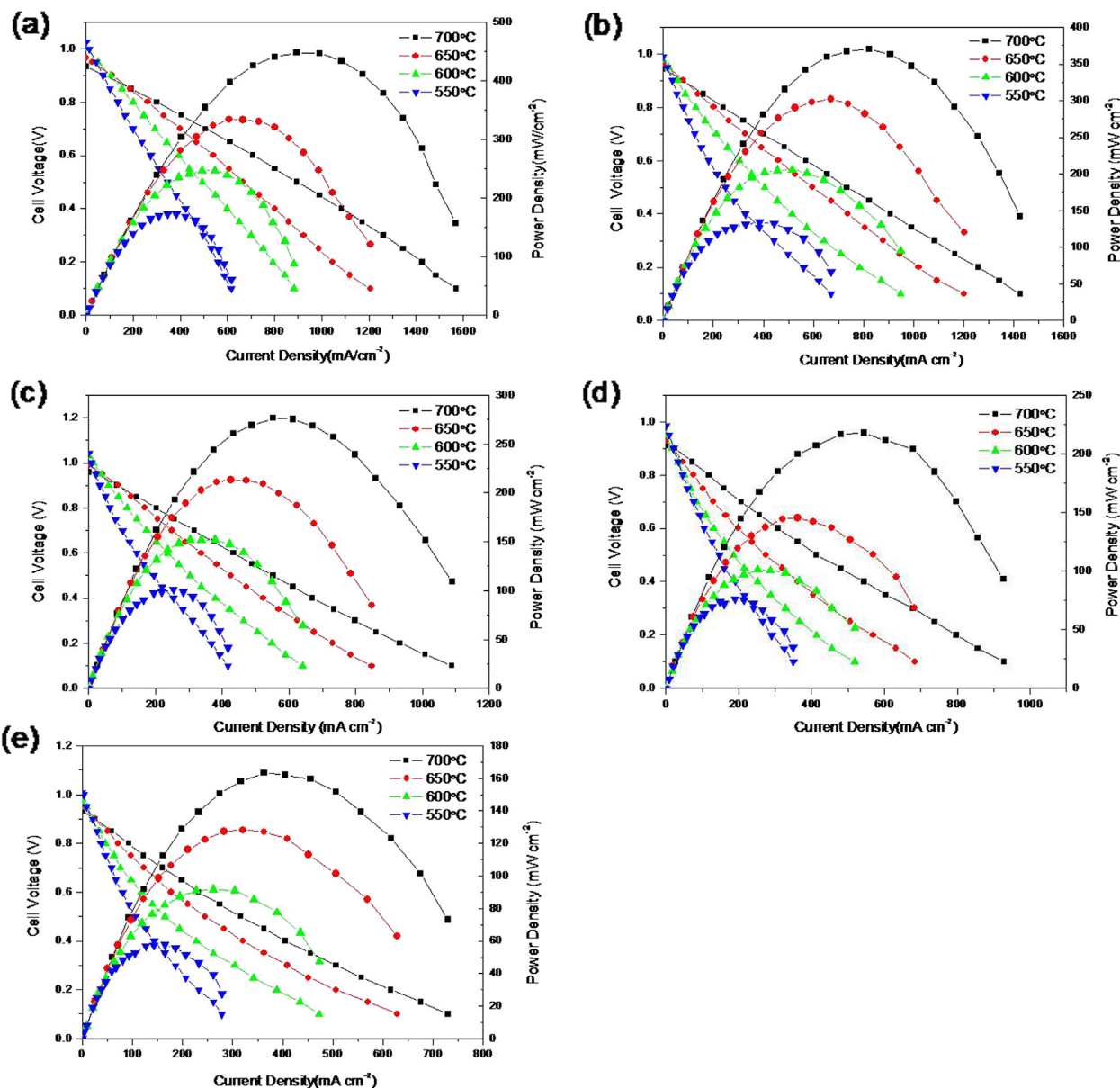


Fig. 4. *I*–*V* curves and power densities of anode-supported single cells measured at different temperatures: (a) BCY single layer electrolyte, (b) ~700 nm BZY/BCY bilayer electrolyte, (c) ~1.7 μm BZY/BCY bilayer electrolyte, (d) ~2.4 μm BZY/BCY bilayer electrolyte, and (e) ~3.6 μm BZY/BCY bilayer electrolyte.

($\lambda = 248$ nm) at an energy density of ~ 3 J cm $^{-2}$ and a repetition rate of 10 Hz. The BCY half-cells were heated to 680 °C with oxygen partial pressure of 5 Pa. Post-annealing at 800 °C for 2 h was used to enhance the crystallinity of the film.

Sm $_{0.5}$ Sr $_{0.5}$ CoO $_{3-\delta}$ –Ce $_{0.8}$ Sm $_{0.2}$ O $_{2-\delta}$ (SSC-SDC) as the cell cathode, which was composed of composite powders mixed with a 10 wt.% ethylcellulose–terpineol binder, was painted on the bilayer electrolytes and then fired at 1000 °C for 3 h to form a complete cell. The cathode area is 0.237 cm 2 . Ag paste was applied on the electrode as a current collector.

2.2. Cell tests

The electrochemical performance characteristics of the cells were evaluated with an Al $_2$ O $_3$ test housing placed inside of a furnace. The cell testing was performed from 550 to 700 °C with humidified hydrogen ($\sim 3\%$ H $_2$ O) as a fuel and atmospheric air as the oxidant. The flow rate of the humidified hydrogen was 25 mL min $^{-1}$. The performance was measured with a DC Electronic Load (ITech Electronics

model IT8511). The resistances of the cell under open circuit conditions were measured with an impedance analyzer (CHI604B, Shanghai Chenhua), and the frequency was swept from 100 kHz to 0.1 Hz.

2.3. Characterization of phase composition and microstructures of the cells

The crystal phases of the BCY electrolyte and BZY/BCY bilayer electrolytes were examined using an X-ray diffractometer (XRD) equipped with Cu K α radiation. The microstructures of the cells were observed with a scanning electron microscope (SEM, JEOL JSM-6700F), and the elemental distribution was determined using energy-dispersive X-ray spectroscopy (EDS).

3. Results and discussion

Fig. 1 presents XRD patterns of the BCY single electrolyte layer and the BZY/BCY bilayer samples. BCY has an orthorhombic

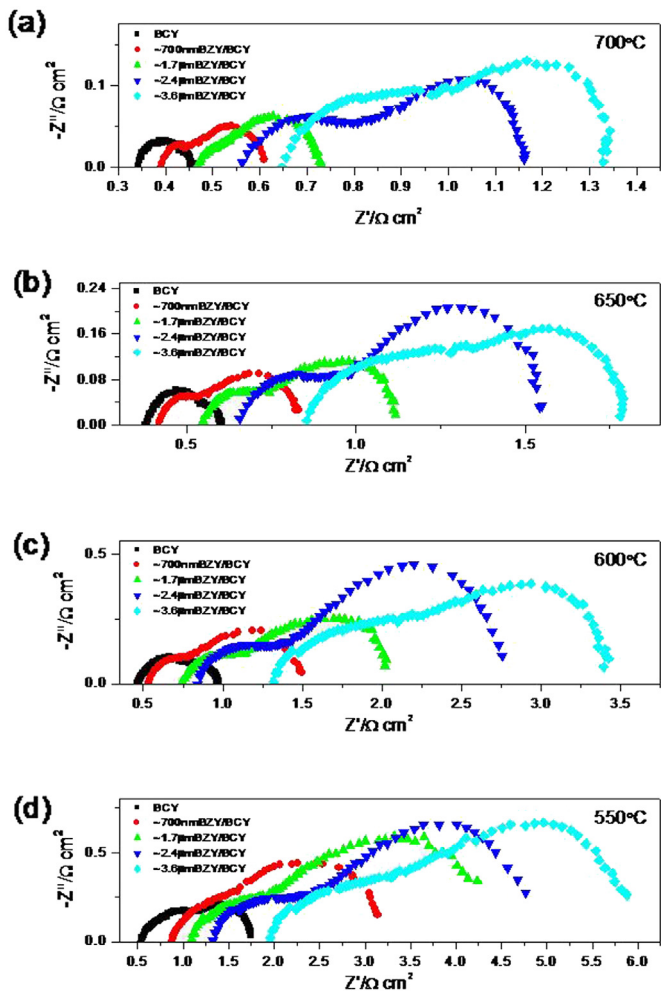


Fig. 5. The electrochemical impedance spectra of the BCY single electrolyte cell and BZY/BCY bilayer electrolyte cells with different the BZY layer thicknesses measured at (a) 700 °C, (b) 650 °C, (c) 600 °C, (d) 550 °C.

perovskite structure as shown in Fig. 1a. The diffraction patterns in Fig. 1b–e depict the cubic reflections of the BZY crystalline structure. The reflections of the two crystalline structures can be grouped into pairs, and each of the pairs corresponds to the same set of Miller indices, which indicates an epitaxial grain by grain growth [14]. The relative densities of the BCY diffraction patterns show a downtrend with increasing BZY layer thickness. No additional reflection lines of unwanted phases, such as the BCY-BZY solid solution compounds, are present in the XRD pattern, which indicates that no interdiffusion between BZY and BCY occurred.

Fig. 2a shows the cross-sectional image of a BZY/BCY bilayer electrolyte sample. The thickness of the BCY electrolyte is $\sim 29 \mu\text{m}$. The BZY layer is $\sim 3.6 \mu\text{m}$ thick. The BZY layer appears to be quite dense, and it adheres well to the BCY electrolyte with no cracks present. Fig. 2b depicts the EDS scans as the sequence: anode/BCY electrolyte/BZY/SSC-SDC cathode cell (from left to right in Fig. 2b). Zr is only present in the BZY layer and no obvious interdiffusion between BCY and BZY can be observed, which is consistent with the above mentioned result from the X-ray analysis. Zr element also appears in BCY electrolyte for a few micrometers which may be caused by the diffusion of Zr in NiO-BZCY. The diffusion only exists near the anode and cannot affect the research of the BZY/BCY bilayer electrolyte.

High chemical stability is critical for the electrolyte materials in HTPCs to ensure a long-term stability, especially when

hydrocarbons are used as fuels [16,17]. In order to investigate the effect of the BZY layers on protecting the chemical stability of the BCY electrolyte, BCY single electrolyte layer and BZY/BCY bilayer samples with different thicknesses of BZY layers (from $\sim 700 \text{ nm}$ to $\sim 3.6 \mu\text{m}$) were separately treated in 100% CO_2 atmosphere at 900 °C for 3 h. The XRD analysis of the CO_2 -treated films was depicted in Fig. 3. The perovskite structure of BCY single layer sample decomposed into BaCO_3 as shown in Fig. 3a. This result indicates that BCY single layer is not stable enough under a CO_2 -containing atmosphere, which is consistent with other reports [18,19]. The X-ray analysis of the treated BZY/BCY bilayer samples shows a changing phenomenon. As depicted in Fig. 3b, the bilayer sample with $\sim 700 \text{ nm}$ thickness of BZY decomposed into BaCO_3 and CeO_2 after exposure to CO_2 -containing atmosphere. The phenomenon is also observed in CO_2 -treated BZY ($\sim 1.7 \mu\text{m}$)/BCY bilayer sample as shown in Fig. 3c. The peaks related to BaCO_3 still exist in the XRD pattern of the BZY ($\sim 2.4 \mu\text{m}$)/BCY sample in Fig. 3d. When the thickness of the BZY layer was increased to $\sim 3.6 \mu\text{m}$, the bilayer sample maintained the perovskite lattice structure in Fig. 3e. It demonstrates that the BZY layer with certain thickness has a sufficient chemical stability against CO_2 , and thus the BZY/BCY bilayer electrolyte is promising as a proton conductor SOFCs electrolyte concerning chemical stability.

Although BZY has a favorable chemical stability against CO_2 atmosphere, the poor proton conductivity [20,21] can influence the electrochemical properties of the BZY/BCY bilayer electrolyte cell. I - V characteristics and power densities of the BCY single electrolyte cell and BZY/BCY bilayer electrolyte cells were measured from 550 to 700 °C. As shown in Fig. 4a, the open circuit voltage (OCV) is 0.933 V for BCY single electrolyte cell at 700 °C. The OCVs of BZY/BCY bilayer electrolyte cells with various thicknesses of BZY layers (from $\sim 700 \text{ nm}$ to $\sim 3.6 \mu\text{m}$) are 0.943, 0.94, 0.91 and 0.934 V at 700 °C, respectively, as depicted in Fig. 4b–e. The high OCV values indicate that both the BCY electrolyte layer and the BZY layers are quite dense. The maximum power densities (MPDs) decline with increasing BZY layer thickness. As shown in Fig. 4a, the MPDs of the BCY single electrolyte ($\sim 29 \mu\text{m}$) cell are 447, 333, 247 and 173 mW cm^{-2} at 700, 650, 600 and 550 °C, respectively. The MPDs are comparable with the values reported for the BaCeO_3 -based electrolyte fuel cells [1,5]. The BZY/BCY bilayer cells reveal a trend towards lower MPDs with increasing BZY layer thickness. For a cell with thinner BZY ($\sim 700 \text{ nm}$)/BCY bilayer electrolyte, as shown in Fig. 4b, the MPDs decrease to 370, 301, 206 and 134 mW cm^{-2} at 700, 650, 600 and 550 °C, respectively. In Fig. 4c, the cell with thicker BZY layer ($\sim 1.7 \mu\text{m}$) shows lower MPDs of 276, 213, 152 and 101 mW cm^{-2} at 700, 650, 600 and 550 °C, respectively. When the BZY layer increases to $\sim 2.4 \mu\text{m}$ thick, the MPDs decrease to 218, 145, 101 and 76 mW cm^{-2} at 700, 650, 600 and 550 °C, respectively, as shown in Fig. 4d. Although the MPDs decrease with increasing BZY layer thickness, they are still higher than or comparable with the reported values for several BaCeO_3 -based fuel cells [1,22–25]. The SOFC with thicker BZY layer ($\sim 3.6 \mu\text{m}$) shows the MPDs of 163, 128, 92 and 58 mW cm^{-2} at 700, 650, 600 and 550 °C, respectively, as shown in Fig. 4e. The MPDs are relatively lower than the other tested bilayer cells. However, the value is still higher than that of the BCY electrolyte-supported bilayer cell [14].

Fig. 5 shows the electrochemical impedance spectra of the BCY electrolyte cell and BZY/BCY bilayer electrolyte cells measured at 700, 650, 600, and 550 °C under open circuit conditions. The first intercept on the real axis at high frequency corresponds to the ohmic resistance (R_o), which includes internal resistance of the electrolyte and electrodes and the contact resistance at the interfaces between the electrodes and the electrolytes and between the electrodes and the current collectors [26]. The difference between the high frequency and the low frequency represents the

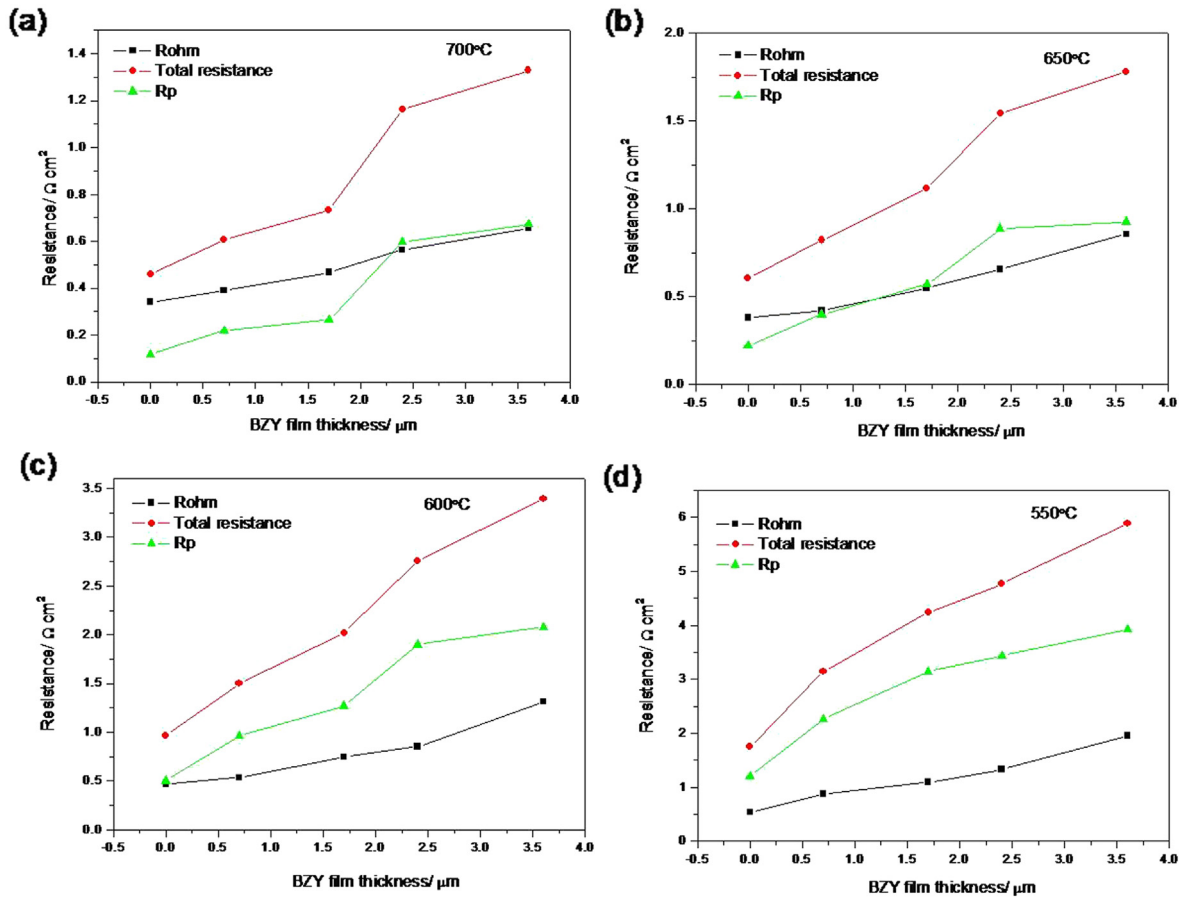


Fig. 6. The values of R_o , R_p and total resistance estimated from impedance spectroscopy measurement as a function of BZY layer thickness at different temperatures: (a) 700 °C, (b) 650 °C, (c) 600 °C, (d) 550 °C.

interfacial polarization resistance (R_p), which is contributed by cathode and anode [27].

The values of R_o , R_p and total resistance estimated from impedance spectroscopy measurement as a function of the BZY thicknesses at different temperatures were plotted in Fig. 6. As shown in Fig. 6a, the ohmic resistances are 0.34, 0.39, 0.47, 0.56 and 0.66 $\Omega\text{ cm}^2$, and the polarization resistances are 0.12, 0.22, 0.26, 0.60 and 0.67 $\Omega\text{ cm}^2$ with BZY layers thicknesses of 0, 0.7, 1.7, 2.4 and 3.6 μm at 700 °C, respectively. When the thickness of the BZY

layer increases to 2.4 μm or even higher, the corresponding values of R_p are higher than those of R_o . In Fig. 6b and c, R_p increases more quickly than R_o at 650 °C and 600 °C, indicating that R_p makes larger contribution to the total resistance. At 550 °C, as shown in Fig. 6d, the ohmic resistances increase to 0.56, 0.88, 1.09, 1.33 and 1.96 $\Omega\text{ cm}^2$, while the polarization resistances increase to 1.20, 2.26, 3.14, 3.43 and 3.92 $\Omega\text{ cm}^2$ with BZY thickness of 0, 0.7, 1.7, 2.4 and 3.6 μm , respectively. R_p becomes the main contribution to the total resistance. The increasing value of R_o results from the increasing

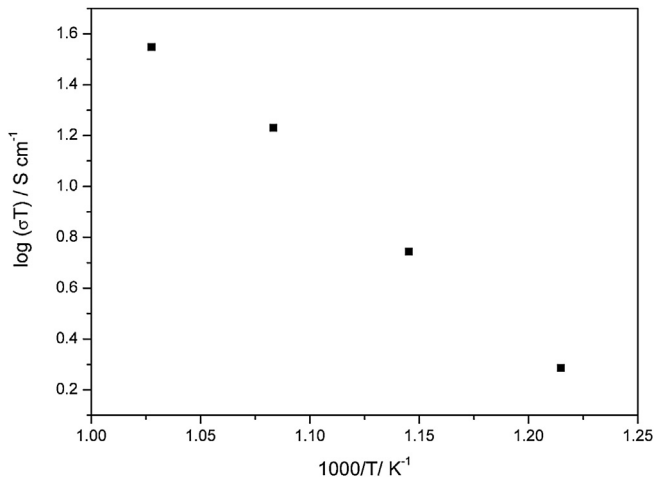


Fig. 7. Conductivity of BZY (~3.6 μm)/BCY electrolyte membrane as a function of temperature under cell testing conditions.

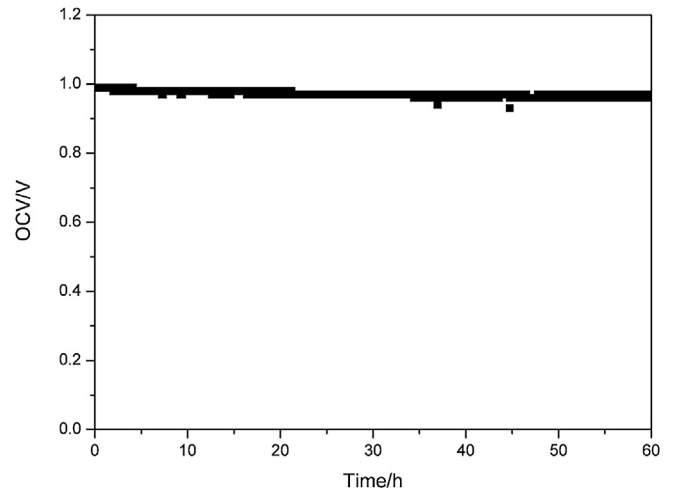


Fig. 8. The OCV of BZY (~3.6 μm)/BCY bilayer electrolyte cell at 600 °C as a function of time with hydrogen (3% H_2O) as the fuel.

thickness of electrolyte and the relatively low conductivity of BZY compared with that of BCY. The high value of R_p is probably due to the electrode materials and interface between the bilayer electrolyte and electrode. Sun et al. [2] have reported that SSC-SDC cathode is easy to peel off the BaZrO₃-based electrolyte film. The poor interface between cathode and electrolyte would hinder charge transfer and current collecting and thus results in high polarization resistance. The similar problem was found and researched at the interface between the Pt and BZY [14]. Besides, after depositing BZY layer, the conductivity of electrolyte layer decreased which influenced charge transfer and increased anode polarization loss. Not only the BZY/cathode interface resistance, but also the BCY/anode resistance was increased after depositing BZY layer. Besides, the resistances increased with the thickness of the BZY layer in the investigated cases. Thus, the decreasing maximum power output with increasing BZY layer thickness can be attributed to the low proton conductivity and poor cathode/electrolyte interface. Further improvement in the interface microstructure is essential for achieving optimum electrochemical performance of BZY/BCY bilayer cell. Considering the results of chemical stability against CO₂ and electrochemical performance, BZY (~3.6 μm)/BCY bilayer electrolyte turns out to be a promising electrolyte without greatly diminishing the electrochemical performance and with favorable chemical stability for proton-conducting SOFCs.

Assuming the ohmic resistance mostly came from the electrolyte, the conductivity of BZY (~3.6 μm)/BCY electrolyte membrane was calculated from the value of R_o . As shown in Fig. 7, the membrane conductivities are 4.83×10^{-3} , 3.71×10^{-3} , 2.41×10^{-3} and 2.07×10^{-3} S cm⁻¹ at 700, 650, 600 and 550 °C, respectively, which are lower than the self-supported BCY membrane of 1.47×10^{-2} S cm⁻¹ at 700 °C [28]. However, the values are comparable with those of anode-supported BaCeO₃-based electrolyte [1,25,29].

The stability of the BZY (~3.6 μm)/BCY bilayer electrolytes fuel cell was evaluated under fuel cell testing conditions. As shown in Fig. 8, the OCV of the cell at 600 °C was recorded as a function of operation time with hydrogen (3% H₂O) as the fuel. The OCV kept stable after 60 h which indicates that the bilayer electrolyte structure was not broken after operating 60 h under open circuit condition.

4. Conclusions

PLD technique has been used in this study to deposit the BZY protecting layer on anode-supported BCY electrolyte SOFCs with the BZY layer thicknesses varied from ~700 nm to ~3.6 μm. The BCY-BZY solid solution compounds were avoided due to the low processing temperatures of the PLD technique. BZY (~3.6 μm)/BCY bilayer electrolyte proves to be stable against 100% CO₂ atmosphere treated at 900 °C. The OCV values of the BZY/BCY bilayer electrolyte cells are 0.933, 0.943, 0.94, 0.91 and 0.934 V with the BZY layer thicknesses of 0, 0.7, 1.7, 2.4 and 3.6 μm at 700 °C, respectively. It indicates that the protecting BZY layers deposited by PLD technique are quite dense. The maximum power densities of 447, 370, 276, 218

and 163 mW cm⁻² are measured with the BZY layer thicknesses of 0, 0.7, 1.7, 2.4 and 3.6 μm at 700 °C, respectively. BZY/BCY bilayer electrolyte exhibits to be a promising proton electrolyte candidate for SOFCs with good chemical stability, favorable proton conductivity and electrochemical performance. The conductivity of the bilayer electrolyte and the power output of the cells are not high enough for intermediate temperature SOFCs, thus further improvement is needed on reducing the bilayer electrolyte/electrode interface resistance and enhancing the protonic conductivity of the bilayer electrolyte.

Acknowledgments

This work was supported by Ministry of Science and Technology of China (grant no: 2012CB215403). The project was also supported by research fund of Key Laboratory for Advanced Technology in Environmental Protection of Jiangsu Province and Anhui Nature Science Foundation.

References

- [1] L. Bi, S. Zhang, S. Fang, Z. Tao, R. Peng, W. Liu, *Electrochem. Commun.* 10 (2008) 1598–1601.
- [2] W. Sun, Z. Zhu, Z. Shi, W. Liu, *J. Power Sources* 229 (2013) 95–101.
- [3] H. Iwahara, T. Esaka, H. Uchida, N. Maeda, *Solid State Ionics* 3–4 (1981) 359–363.
- [4] L. Bi, E. Fabbri, Z. Sun, E. Traversa, *Energy Environ. Sci.* 4 (2011) 1352–1357.
- [5] C. Zuo, S. Zha, M. Liu, M. Hatano, M. Uchiyama, *Adv. Mater.* 18 (2006) 3318.
- [6] K.D. Kreuer, *Annu. Rev. Mater. Res.* 33 (2003) 333–359.
- [7] E. Fabbri, D. Pergolesi, E. Traversa, *Chem. Soc. Rev.* 39 (2010) 4355–4369.
- [8] D. Pergolesi, E. Fabbri, A. D'Epifanio, E. Di Bartolomeo, A. Tebano, S. Sanna, S. Licocchia, G. Balestrino, E. Traversa, *Nat. Mater.* 9 (2010) 846–852.
- [9] Y. Yamazaki, R. Hernandez-Sanchez, S.M. Haile, *Chem. Mater.* 21 (2009) 2755–2762.
- [10] K.D. Kreuer, *Solid State Ionics* 125 (1999) 285–302.
- [11] K.D. Kreuer, S. Adams, W. Munch, A. Fuchs, U. Klock, J. Maier, *Solid State Ionics* 145 (2001) 295–306.
- [12] J.H. Joo, G.M. Choi, *Solid State Ionics* 177 (2006) 1053–1057.
- [13] D. Pergolesi, E. Fabbri, E. Traversa, *Electrochem. Commun.* 12 (2010) 977–980.
- [14] E. Fabbri, D. Pergolesi, A. D'Epifanio, E. Di Bartolomeo, G. Balestrino, S. Licocchia, E. Traversa, *Energy Environ. Sci.* 1 (2008) 355–359.
- [15] W. Sun, Y. Jiang, Y. Wang, S. Fang, Z. Zhu, W. Liu, *J. Power Sources* 196 (2011) 62–68.
- [16] Y. Liu, Y. Guo, R. Ran, Z. Shao, *J. Membr. Sci.* 415 (2012) 391–398.
- [17] E. Fabbri, L. Bi, D. Pergolesi, E. Traversa, *Adv. Mater.* 24 (2012) 195–208.
- [18] Y. Guo, Y. Lin, R. Ran, Z. Shao, *J. Power Sources* 193 (2009) 400–407.
- [19] S.M. Haile, G. Staneff, K.H. Ryu, *J. Mater. Sci.* 36 (2001) 1149–1160.
- [20] H.-I. Ji, B.-K. Kim, J.H. Yu, S.-M. Choi, H.-R. Kim, J.-W. Son, H.-W. Lee, J.-H. Lee, *Solid State Ionics* 203 (2011) 9–17.
- [21] J. Tong, D. Clark, L. Bernau, M. Sanders, R. O'Hayre, *J. Mater. Chem.* 20 (2010) 6333–6341.
- [22] L. Bi, Z. Tao, W. Sun, S. Zhang, R. Peng, W. Liu, *J. Power Sources* 191 (2009) 428–432.
- [23] Z. Tao, Z. Zhu, H. Wang, W. Liu, *J. Power Sources* 195 (2010) 3481–3484.
- [24] L. Bi, S. Zhang, B. Lin, S. Fang, C. Xia, W. Liu, *J. Alloys Compd.* 473 (2009) 48–52.
- [25] K. Xie, R. Yan, X. Chen, D. Dong, S. Wang, X. Liu, G. Meng, *J. Alloys Compd.* 472 (2009) 551–555.
- [26] F. Zhao, A.V. Virkar, *J. Power Sources* 141 (2005) 79–95.
- [27] C.R. Xia, W. Rauch, W. Wellborn, M.L. Liu, *Electrochem. Solid State Lett.* 5 (2002) A217–A220.
- [28] E. Fabbri, A. D'Epifanio, E. Di Bartolomeo, S. Licocchia, E. Traversa, *Solid State Ionics* 179 (2008) 558–564.
- [29] B. Lin, M. Hu, J. Ma, Y. Jiang, S. Tao, G. Meng, *J. Power Sources* 183 (2008) 479–484.